Computer Assisted Methods in Engineering and Science, **23**: 109–132, 2016.

The discontinuous Galerkin method with higher degree finite difference compatibility conditions and arbitrary local and global basis functions

Jan Jaśkowiec
Cracow University of Technology, Faculty of Civil Engineering
Institute for Computational Civil Engineering
Warszawska 24, 31-155 Kraków, Poland
e-mail: j.jaskowiec@L5.pk.edu.pl

This paper focuses on the discontinuous Galerkin (DG) method in which the compatibility condition on the mesh skeleton and Dirichlet boundary condition on the outer boundary are enforced with the help of one-dimensional finite difference (FD) rules, while in the standard approach those conditions are satisfied by the penalty constraints. The FD rules can be of arbitrary degree and in this paper the rules are applied up to fourth degree. It is shown that the method presented in this paper gives better results in comparison to the standard version of the DG method. The method is based on discontinuous approximation, which means that it can be constructed using arbitrary local basis functions in each finite element. It is quite easy to incorporate some global basis functions in the approximation field and this is also shown in the paper. The paper is illustrated with a couple of two-dimensional examples.

Keywords: discontinuous Galerkin method, finite difference, compatibility condition, approximation basis.

1. Introduction

This paper deals with a discontinuous finite element method that is known in the literature as the discontinuous Galerkin (DG) method. In this method, the approximation field is discontinuous along the mesh skeleton, i.e., the boundaries between adjacent finite elements. This is due to the fact that in this method the approximation is constructed separately for each finite element using standard shape functions. The approximation continuity between neighboring cells is not guaranteed. In spite of the lack of continuity in the approximation fields the DG method is usually used to find the solutions of continuous problems. Consistency of the final solution is enforced by compatibility conditions that are derived using different techniques. Commonly applied techniques are mortar or Nitsche's methods. In the mortar methods, additional unknowns are used to set the relation between different domains along the common interface. In most cases, the compatibility conditions are enforced by means of Lagrange multipliers, e.g., [5, 19, 29]. The main drawback of mortar methods is that the matrix of discrete system of equations is no longer positive-definite. The Nitsche's method [37] is a penalty-like approach in which a normal flux on the inter-element interface is combined with penalty parameter, e.g., [40]. In the literature three versions of the Nitsche's approach in DG the method are used, so the following DG schemes arise: i) symmetric interior penalty Galerkin (SIPG) [50], ii) nonsymmetric interior penalty Galerkin (NIPG) [42], and iii) incomplete interior penalty Galerkin (IIPG) [13, 48]. The IIPG scheme is in fact a pure penalty method presented for example in [1]. An alternative approach is proposed in [24] in which a negligibly thin layer of material between adjacent elements is defined. Subsequently, on that thin layer special finite elements are defined, which guarantee continuity of approximation.

In this paper the compatibility condition is based on the finite difference (FD) relations which can be of second or fourth degrees. However, higher orders can be applied if necessary. Quite similar ap-

proach is applied for Dirichlet boundary conditions, and in this case the FD relations are of first, second or fourth degree. In order to distinguish the version of DG method presented in this paper from the standard discontinuous Galerkin (SDG) method (i.e., interior penalty discontinuous Galerkin method [2]) the concept is called a discontinuous Galerkin with finite difference (DGFD) method.

The approximation over each finite element (or cell in short) is usually based on standard or hierarchical shape functions [27, 28, 40]. This means that a set of nodes is defined in each cell and these nodes are not shared with neighboring cells. In the DG method also another approach is possible, in which the approximation in each cell is based not on shape functions but on polynomial basis functions taken from Taylor's expansion [31, 32] or usage of other basis functions is possible [52]. In this paper the idea is pursued further to extend it to arbitrary basis functions such as, for example, radial basis functions. Furthermore, in this work the local approximation is enriched by the global one. The global approximation is based on a set of global basis functions. The global functions can be locally scaled in each cell by additional local degrees of freedom or, on the other hand, the global functions can be scaled by global degrees of freedom. The global functions in this paper can be spanned over all elements in the domain or their support can be limited to an arbitrary set of cells. The discontinuous Galerkin method, in the version presented in this paper, gives a great flexibility in *a priori* adjusting the approximation field to a considered problem. For example, global special functions known from fracture mechanics, can be applied, but this kind of problem is out of scope of this work. The technique of adding global functions to approximation is known in the literature as an extended method, i.e., the extended finite element method (XFEM) [25, 35], extended discontinuous Galerkin (XDG) method [22, 30] or generalized finite element method (GFEM) [15, 46, 47]. However, a technique presented in this paper is much easier in comparison to these above mentioned extended methods. The criteria for choosing a global function stay the same as in the XFEM, XDG and GFEM.

In this paper the DGFD method is applied to a scalar elliptic problem in three-dimensional (3D) domains. However, the examples presented in this paper are limited to two-dimensional cases. A typical example of scalar elliptic problem is heat transport, which has been chosen here for the analysis. Although the paper is focused on elliptic problems, the approach can be directly applied to other kinds of problems.

The origin of the discontinuous Galerkin method (DG) goes back to the 1970s [39], when the method was introduced and applied to the numerical solution of a nuclear transport PDE problem. The method has been subsequently explored by many researchers. Since the 1970s numerous DG methods have been developed, for example: the total variation bounded Runge-Kutta DG [4, 9–11, 55], the local DG method [8, 12, 26], the interior penalty (IPDG) method, the mixed DG method, the central DG method, the hybridizable DG method, the space-time DG method, the positivity-preserving DG method, and many others. The DG method has also been applied to some particular problems in structural mechanics, e.g., [17, 23, 38], in fracture modelling [43–45] or in the modelling of phase flow in porous media [18, 41]. The DG method has been found sufficiently flexible for *hp* refinement and has been extended to be applied to various partial differential equations, e.g., [6, 7, 20, 21, 56]. A different approach to DG method is presented in [24], where the compatibility conditions are constructed by non-zero skeleton width.

The following Sec. 2 presents the equations of the elliptic problem for which the DGFD method is formulated. The concept of how the compatibility and boundary conditions can be satisfied using the FD equations is described in Sec. 3. Section 4 deals with local and global approximations in the DGFD method and the linear set of equation for the DGFD method is derived. The presented approach is illustrated with a couple of examples in Sec. 5. The paper ends with some conclusions.

2. Mathematical formulation of DGFD method

The DGFD method is presented for a scalar elliptic problem with a physical interpretation of stationary heat transport. The problem is defined in the domain V with outer boundary S. The

problem starts with the well-known local form of energy balance equation, the Fourier law as well as Dirichlet and Neumann boundary conditions. The problem is formulated as follows: find the continuous temperature field Θ that satisfies the following relationships:

$$\begin{aligned} &\operatorname{div}\mathbf{q} - r = 0 && \text{in } V,\\ &\mathbf{q} = -k\nabla\Theta && \text{in } V,\\ &\Theta = \widehat{\Theta} && \text{on } S_\Theta,\\ &\mathbf{q}\cdot\mathbf{n} = \widehat{h} && \text{on } S_q, \end{aligned} \tag{1}$$

where $\mathbf{q}$ is the heat flux vector, r is the heat source density, k is the heat conductivity parameter for a thermally isotropic material, and $\widehat{\Theta}$ and $\widehat{h}$ are prescribed values of temperature and heat flux, respectively, S_Θ is the part of S where temperature $\widehat{\Theta}$ is prescribed, S_q is the part of S where heat flux $\widehat{h}$ is prescribed, and $\mathbf{n}$ is the unit vector normal to the outer boundary. The heat flux vector is connected with the temperature field by means of Fourier's law written in Eq. $(1)_2$.

The considered domain is structured by a finite element mesh. The mesh consists of a set of cells and inter-element boundaries. The set of inter-element boundary segments is called the mesh skeleton S_s, or skeleton in short. The discontinuous Galerkin method is based on the discontinuous approximation with the discontinuity on the skeleton. The discontinuity has to be regarded in the global formulation of the problem defined in Eq. (1), where the integration by parts is performed. In the calculations, the unit vector normal to skeleton $\mathbf{n}^s$ is needed, which is called in this paper the skeleton normal. The orientation of the vector is arbitrary in the sense that it can be directed to either of the adjacent cells.

In the approach presented in this paper the definition of the jump and the mid-value operators is needed, which are defined in the direction normal to the skeleton, namely

$$[\![f]\!] = \lim_{\epsilon\to 0}[\![f]\!]_\epsilon, \qquad \langle f\rangle = \lim_{\epsilon\to 0}\langle f\rangle_\epsilon, \tag{2}$$

where

$$[\![f]\!]_\epsilon = f(\mathbf{x}+\epsilon\,\mathbf{n}^s) - f(\mathbf{x}-\epsilon\,\mathbf{n}^s), \qquad \langle f\rangle_\epsilon = 0.5\,\left(f(\mathbf{x}+\epsilon\,\mathbf{n}^s) + f(\mathbf{x}-\epsilon\,\mathbf{n}^s)\right), \tag{3}$$

where ϵ is the auxiliary parameter.

It is a well-known property that the jump of two functions product can be expressed as follows

$$[\![fg]\!] = [\![f]\!]\,\langle g\rangle + \langle f\rangle\,[\![g]\!]. \tag{4}$$

The discontinuous Galerkin method starts with the global formulation of the considered problem, defined in Eq. (1), with the test function v

$$\int_V v\,\operatorname{div}\mathbf{q}\,\mathrm{d}V - \int_V v\,r\,\mathrm{d}V = 0 \qquad \forall\, v. \tag{5}$$

After integration by parts, Eq. (5) changes into

$$\int_V \operatorname{div}(v\,\mathbf{q})\,\mathrm{d}V - \int_V \nabla v\cdot\mathbf{q}\,\mathrm{d}V - \int_V v\,r\,\mathrm{d}V = 0. \tag{6}$$

The first integral in Eq. (6) is over the domain volume where its integrand is just a divergence. In the case when $(v\,\mathbf{q})$ is continuous in V the integral is equal to an integral along the outer bondary. Since the function $(v\,\mathbf{q})$ is discontinuous on the mesh skeleton S_s the integral, regarding

the definition in Eq. (2), is equal to the integral over the outer boundary minus the integral over the skeleton, i.e.,

$$\int_V \operatorname{div}(v\,\mathbf{q})\,\mathrm{d}V = \int_S v\,\mathbf{q}\cdot\mathbf{n}\,\mathrm{d}S - \int_{S_s} [\![v\,\mathbf{q}]\!]\cdot\mathbf{n}^s\,\mathrm{d}S. \tag{7}$$

On the basis of Eq. (4), Eq. (7) can be rewritten as

$$\int_V \operatorname{div}(v\,\mathbf{q})\,\mathrm{d}V = \int_S v\,\mathbf{q}\cdot\mathbf{n}\,\mathrm{d}S - \int_{S_s} [\![v]\!]\,\langle\mathbf{q}\rangle\cdot\mathbf{n}^s\,\mathrm{d}S - \int_{S_s} \langle v\rangle\,[\![\mathbf{q}]\!]\cdot\mathbf{n}^s\,\mathrm{d}S. \tag{8}$$

There is no heat source on the skeleton. That is why the jump of the heat flux in the skeleton normal direction is zero, and this means that the heat flux vector is continuous in the normal direction

$$[\![\mathbf{q}]\!]\cdot\mathbf{n}^s = 0 \quad\Rightarrow\quad \langle\mathbf{q}\rangle\cdot\mathbf{n}^s = \mathbf{q}\cdot\mathbf{n}^s \qquad \text{on} \quad S_s. \tag{9}$$

The integral over outer boundary from Eq. (8) can be expressed as the sum over S_Θ and S_q. Subsequently, the Neumann boundary condition from Eq. (1) can be applied on S_q

$$\int_S v\,\mathbf{q}\cdot\mathbf{n}\,\mathrm{d}S = \int_{S_q} v\,\widehat{h}\,\mathrm{d}S + \int_{S_\Theta} v\,\mathbf{q}\cdot\mathbf{n}\,\mathrm{d}S. \tag{10}$$

Taking into account equations from (8) to (10), Eq. (6) is written in the following form:

$$\int_{S_q} v\,\widehat{h}\,\mathrm{d}S + \int_{S_\Theta} v\,\mathbf{q}\cdot\mathbf{n}\,\mathrm{d}S - \int_{S_s} [\![v]\!]\,\mathbf{q}\cdot\mathbf{n}^s\,\mathrm{d}S - \int_V \nabla v\cdot\mathbf{q}\,\mathrm{d}V - \int_V v\,r\,\mathrm{d}V = 0. \tag{11}$$

The heat flux vector is expressed by Fourier's law, i.e., $\mathbf{q} = -k\nabla\Theta$, and then Eq. (11) changes into

$$\int_{S_q} v\,\widehat{h}\,\mathrm{d}S - \int_{S_\Theta} k\,v\,\nabla\Theta\cdot\mathbf{n}\,\mathrm{d}S + \int_{S_s} k\,[\![v]\!]\,\nabla\Theta\cdot\mathbf{n}^s\,\mathrm{d}S + \int_V k\,\nabla v\cdot\nabla\Theta\,\mathrm{d}V - \int_V v\,r\,\mathrm{d}V = 0. \tag{12}$$

Up to now the problem formulation presented in Eq. (12) is common for the SDG and DGFD methods. The main difference between these two methods lies in approximation of $\nabla\Theta\cdot\mathbf{n}^s$ on S_s. In the SDG method, this gradient is set as mean value of the gradient values on both sides of the skeleton and the penalty component is added to the formulation. In the DGFD method, the temperature gradient is approximated using the FD rules, what is presented in the subsequent section.

3. Compatibility and boundary conditions

In Eq. (12), the third component – the value of the temperature gradient in the skeleton normal direction has to be evaluated. Such a value cannot be said straightforwardly in the DG methods. And also in the finite element method (FEM) it would not be easy to evaluate this value, but in contrast to the FEM, in the DG methods $\nabla\Theta\cdot\mathbf{n}^s$ on S_s have to be evaluated. In the SDG approach the following evaluation on S_s is applied: $\nabla\Theta\cdot\mathbf{n}^s = \langle\nabla\Theta\rangle\cdot\mathbf{n}^s$, what is not coherent with relationships in Eq. (9). In the hybridized DG (HDG) method [36], such a problem is solved by using additional degrees of freedom on the mesh skeleton. In this paper, the alternative method is proposed that uses the FD rules on the mesh skeleton to enforce continuity of the final solution and on the outer Dirichlet boundary to enforce boundary conditions.

In this section, the compatibility and boundary conditions based on the FD relationships of various degrees are presented. The FD equations are derived using the points belonging to a line perpendicular to S_s which is identified by $\mathbf{n}^s$. Any point $\mathbf{x}$ that is close to the skeleton segment can be located in space with the help of point $\mathbf{x}_d$ belonging to the skeleton and the skeleton normal direction, i.e.,

$$\mathbf{x} = \mathbf{x}_d + \beta\,\mathbf{n}^s, \tag{13}$$

where β is an auxiliary scalar parameter. This is illustrated in Fig. 1. Subsequently, the temperature at point $\mathbf{x}$ can be written in the following way:

$$\Theta(\mathbf{x}) = \Theta(\mathbf{x}_d + \beta\,\mathbf{n}^s) = \Theta_d(\beta), \tag{14}$$

where $\Theta_d(\beta)$ describes the temperature at distance β from the point $\mathbf{x}_d \in S_s$ in the normal direction to S_s.

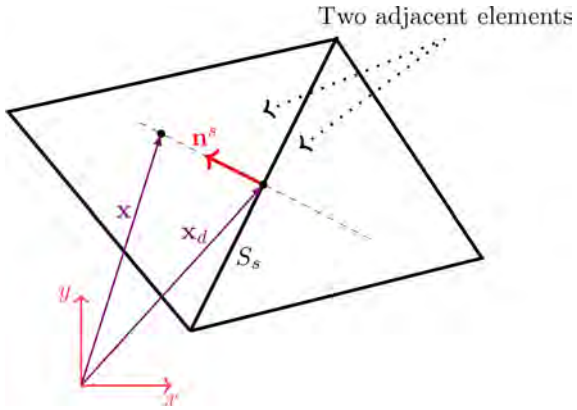

Fig. 1. Location of point $\mathbf{x}$ in relation to point $\mathbf{x}_d \in S_s$.

The derivative of temperature in the $\mathbf{n}^s$ direction can be now expressed by the first derivative of Θ_d

$$\nabla\Theta \cdot \mathbf{n}^s = \Theta_d'. \tag{15}$$

Equation (12) requires a temperature gradient inside the cells (the fourth integral), on the skeleton (the third integral) and on the outer boundary (the second integral). Inside the cells that gradient is calculated in a standard way, which means with the help of approximations inside those cells. Another technique has to be used for the gradient on the skeleton since the temperature approximation is not continuous there. A similar situation is in the case of the outer boundary because the temperature gradient has also to be approximated where the Dirichlet boundary condition is used. In both the cases the FD equations of various degrees are used to solve the problem. In Appendix A all finite difference relationships are derived that are subsequently applied in this section.

On the basis of Eq. (15) the calculation of the temperature derivative on the skeleton in the skeleton normal direction is equivalent to the calculation of the first derivative of Θ_d at the origin of the local coordinate set, i.e.,

$$\nabla\Theta \cdot \mathbf{n}^s = \Theta_d'(0) \qquad \text{on} \quad S_s. \tag{16}$$

On the basis of Eq. (A3) of Appendix A the value of $\Theta_d'(0)$ can be evaluated by the second-degree FD equation with the help of temperature values at distance w from the skeleton segment, see Fig. 2

$$\Theta_d'(0) = \frac{1}{2w}\left(\Theta(w) - \Theta(-w)\right). \tag{17}$$

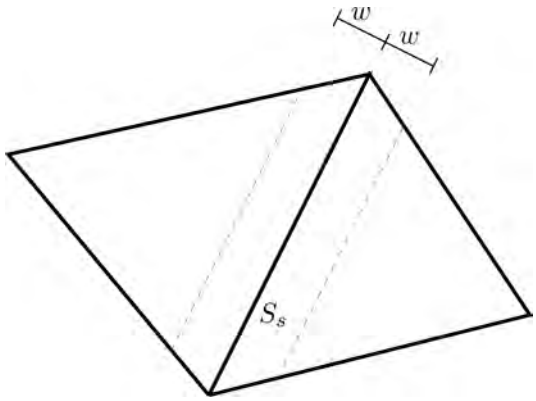

Fig. 2. Distance w from mesh skeleton used for FD relationships.

Now the temperature normal derivative on S_s can be approximated by the following FD relationships:

$$\nabla\Theta\cdot\mathbf{n}^s=\frac{1}{2w}\left(\Theta(\mathbf{x}_d+w\,\mathbf{n}^s)-\Theta(\mathbf{x}_d-w\,\mathbf{n}^s)\right)=\frac{[\![\Theta]\!]_w}{2w}\qquad\text{on}\quad S_s. \tag{18}$$

For a better evaluation of the temperature normal derivative the fourth-degree FD rule can be used according to Eq. (A6). In this case, the normal derivative has a more complicated form

$$\begin{aligned}\nabla\Theta\cdot\mathbf{n}^s&=\frac{3}{4w}\left(\Theta(\mathbf{x}_d+w\,\mathbf{n}^s)-\Theta(\mathbf{x}_d-w\,\mathbf{n}^s)\right)-\frac{1}{4}\left(\nabla\Theta(\mathbf{x}_d+w\,\mathbf{n}^s)+\nabla\Theta(\mathbf{x}_d-w\,\mathbf{n}^s)\right)\cdot\mathbf{n}^s\\&=\frac{3}{2}\cdot\frac{[\![\Theta]\!]_w}{2w}-\frac{1}{2}\cdot\langle\nabla\Theta\rangle_w\cdot\mathbf{n}^s\qquad\text{on}\quad S_s.\end{aligned} \tag{19}$$

In a similar manner, the temperature normal derivative on the outer boundary can be approximated. In this paper the FD approximations of first, second or fourth degrees are used which are based on Eqs. (A8), (A11) or (A14) of Appendix A, respectively. In consequence, the FD approximations on S_Θ take the following forms:

$$\nabla\Theta\cdot\mathbf{n}=\frac{\widehat{\Theta}-\Theta(\mathbf{x}_w)}{w}\qquad\text{1st degree,} \tag{20}$$

$$\nabla\Theta\cdot\mathbf{n}=2\cdot\frac{\widehat{\Theta}-\Theta(\mathbf{x}_w)}{w}-\nabla_n\Theta(\mathbf{x}_w)\qquad\text{2nd degree,} \tag{21}$$

$$\nabla\Theta\cdot\mathbf{n}=6\cdot\frac{\widehat{\Theta}-\Theta(\mathbf{x}_{2w})}{2w}-4\nabla_n\Theta(\mathbf{x}_w)-\nabla_n\Theta(\mathbf{x}_{2w})\qquad\text{4th degree,} \tag{22}$$

where $\mathbf{x}_w=\mathbf{x}-w\,\mathbf{n}$, $\mathbf{x}_{2w}=\mathbf{x}-2\,w\,\mathbf{n}$ and $\nabla_n\Theta=\nabla\Theta\cdot\mathbf{n}$. The graphical illustrations of Eqs. (19) and (21) are presented in Fig. 3.

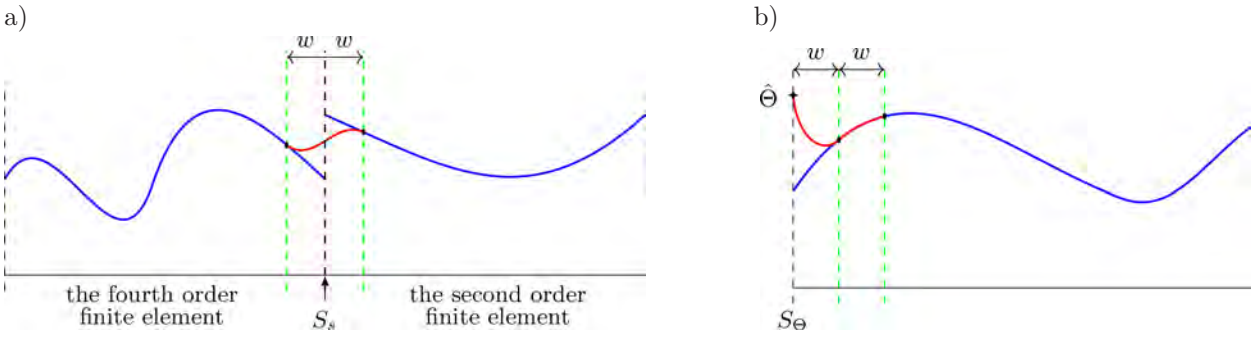

Fig. 3. Graphical illustration of Eqs. (19) and (21) in (a) and (b), respectively. The derivatives of Θ on S_s and S_Θ are taken from the red curve.

Finally Eq. (12) changes into the following formula, where the FD Eqs. (19) and (22) are used

$$\int_{S_q} v\,\widehat{h}\,\mathrm{d}S - \int_{S_\Theta} 3\frac{k}{w} v\widehat{\Theta}\,\mathrm{d}S + \int_{S_\Theta} 3\frac{k}{w} v\Theta(\mathbf{x}_{2w})\,\mathrm{d}S + \int_{S_\Theta} 4\,kv\nabla_n\Theta(\mathbf{x}_w)\,\mathrm{d}S + \int_{S_\Theta} kv\nabla_n\Theta(\mathbf{x}_{2w})\,\mathrm{d}S + \int_{S_s} \frac{3\,k}{4\,w}[\![v]\!][\![\Theta]\!]_w\,\mathrm{d}S - \int_{S_s} \frac{k}{2}[\![v]\!]\mathbf{n}^s\cdot\langle\nabla\Theta\rangle_w\,\mathrm{d}S + \int_V k\,\nabla v\cdot\nabla\Theta\,\mathrm{d}V - \int_V v\,r\,\mathrm{d}V = 0. \quad (23)$$

When we want to use other FD equations on S_s or S_Θ, Eq. (23) has to be accordingly adjusted. Equation (23) can be written in the form of equality of bilinear and linear forms:

$$A(\Theta, v) = F(v), \qquad \forall v, \quad (24)$$

where

$$A(\Theta, v) = \int_V k\nabla v\cdot\nabla\Theta\,\mathrm{d}V + \frac{3}{4}\int_{S_s}\frac{k}{w}[\![v]\!][\![\Theta]\!]_w - \frac{1}{2}\int_{S_s} k[\![v]\!]\,\mathbf{n}^s\cdot\langle\nabla\Theta\rangle_w\,\mathrm{d}S + 3\int_{S_\Theta}\frac{k}{w}v\Theta(\mathbf{x}_{2w})\,\mathrm{d}S + 4\int_{S_\Theta} kv\nabla_n\Theta(\mathbf{x}_w)\,\mathrm{d}S + \int_{S_\Theta} kv\nabla_n\Theta(\mathbf{x}_{2w})\,\mathrm{d}S, \quad (25)$$

$$F(v) = \int_V v\,r\,\mathrm{d}V - \int_{S_q} v\,\widehat{h}\,\mathrm{d}S + 3\int_{S_\Theta}\frac{k}{w}v\widehat{\Theta}\,\mathrm{d}S. \quad (26)$$

For comparison, the corresponding equations in the SDG method are as follows:

$$A(\Theta, v) = \int_V k\nabla v\cdot\nabla\Theta\,\mathrm{d}V + \int_{S_s}\sigma\,[\![v]\!][\![\Theta]\!] - \int_{S_s} k[\![v]\!]\,\mathbf{n}^s\cdot\langle\nabla\Theta\rangle\,\mathrm{d}S + \int_{S_\Theta}\sigma v\Theta\,\mathrm{d}S, \quad (27)$$

$$F(v) = \int_V v\,r\,\mathrm{d}V - \int_{S_q} v\,\widehat{h}\,\mathrm{d}S + \int_{S_\Theta}\sigma\,v\widehat{\Theta}\,\mathrm{d}S, \quad (28)$$

where σ is the penalty parameter. It can be noticed that in the DGFD method in the integrals along the mesh skeleton the values of temperatures or gradients are taken from insides of aligned elements. On the contrary, in the SDG method such values are calculated just on the edges of aligned elements.

4. Discontinuous approximation

In the standard FEM the approximation in a finite element cell is based on shape functions that are constructed on a set of nodes in the cell. The same shape functions are applied in the SDG method, but in this case the finite elements do not share their nodes.

In the approach presented in this paper no shape functions are needed. Instead, for each element the local approximation is constructed by a set of local basis functions. The basis functions are called local here since the functions are defined in the local coordinates associated with each cell. In consequence no nodes are needed in the elements and a set of mathematical degrees of freedom are used to scale the local basis functions. The cell geometry in the finite element mesh is defined by a set of vertices and the definition of cell geometry is independent of the approximation in this cell. In the case of domains with curved boundaries the finite elements cells with curved edges can be used. In such a case the transformation to reference elements can be applied using standard procedures known from the FEM. Then, the second-order Lagrange shape functions may be used to perform the transformation, keeping in mind that the approximation is constructed independently

of the transformation. For the DGFD method the calculations on the reference elements are more complicated than in the FEM since the transformations have to cope with integrals along the mesh skeleton and outer boundary, and this is out of scope of this paper. In the DGFD method not only the local basis functions but also global basis functions can be used in the approximation. The global basis functions are meant here to be defined in the global coordinates. With the help of the global functions some global properties can be included in the approximation. A global basis function can be added to the approximation in two ways: i) the function is scaled locally in each cell by additional local degrees of freedom, ii) the function is scaled globally by a global degree of freedom associated with the mesh. Consequently the final approximation is a superposition of three kinds of approximations, namely:

1. *local-local* – where the linear combination of local basis functions with local degrees of freedom is used,
2. *global-local* – the global basis functions are scaled by additional finite element degrees of freedom,
3. *global-global* – in this case the global basis functions are scaled by global degrees of freedom.

The usage of the global functions in the approximation is similar to the partition of unity approach [3, 34], generalized FEM [47] or extended FEM [35]. The local basis functions have their supports limited to their cells. On the other hand, the support of each global function is spanned over all the cells or over a group of the cells.

The combined local-global approximation written for an e-th element has the following form:

$$\Theta^e(\mathbf{x}) = \sum_{i=1}^{n_e} b_i^e(\mathbf{x})\check{\Theta}_i^e + \sum_{j=1}^{n_{ge}} \beta_j^e(\mathbf{x})\check{\Theta}_j^{ge} + \sum_{k=1}^{n_g} \gamma_k(\mathbf{x})\check{\Theta}_k^g = \mathbf{b}^e\,\check{\boldsymbol{\Theta}}^e + \boldsymbol{\beta}\,\check{\boldsymbol{\Theta}}^{ge} + \boldsymbol{\gamma}\,\check{\boldsymbol{\Theta}}^g\,, \quad \mathbf{x} \in V^e, \tag{29}$$

where $\mathbf{b}^e$ is the vector of local basis functions (LBF) for the e-th cell, $\check{\boldsymbol{\Theta}}^e$ is a vector of local degrees of freedom for local basis functions in the e-th cell, $\boldsymbol{\beta}$ is a vector of global functions locally scaled (GBFL), $\check{\boldsymbol{\Theta}}^{ge}$ is a vector of local degrees of freedom for global basis functions for the e-th cell, $\boldsymbol{\gamma}$ is a vector of global basis of functions (GBF) that are globally scaled, and $\check{\boldsymbol{\Theta}}^g$ is a vector of global degrees of freedom. The degrees of freedom in Eq. (29) are purely mathematical and do not have any physical meaning.

The choice of the local basis functions for each cell is quite arbitrary. For example, they can be Lagrange shape functions which are used in SDG. On the other hand they, for instance, can be based on a Taylor expansion, like in [32, 33, 49, 51]. The local basis functions can be polynomial as well as other functions which are locally defined. The choice of the local basis functions is the user's choice and it may depend on the problem under consideration. On the other hand, the criteria for choosing global basis functions can be, for example, a kind of solution known *a priori*, for problem in L-shaped domain, e.g., [16] or a domain with a crack [25].

In Eq. (29) the approximation for a one element cell is written. It can be rewritten as an approximation for the whole domain

$$\Theta = \boldsymbol{\Phi}\check{\boldsymbol{\Theta}}, \qquad \mathbf{x} \in V, \tag{30}$$

where

$$\begin{aligned} \boldsymbol{\Phi} &= \begin{bmatrix} s^1\mathbf{b}^1 & s^2\mathbf{b}^2 & \dots & s^E\mathbf{b}^E & s^1\boldsymbol{\beta} & s^2\boldsymbol{\beta} & \dots & s^E\boldsymbol{\beta} & \boldsymbol{\gamma} \end{bmatrix}, \\ \check{\boldsymbol{\Theta}}^{\mathrm{T}} &= \begin{bmatrix} \check{\boldsymbol{\Theta}}^{1^{\mathrm{T}}} & \check{\boldsymbol{\Theta}}^{2^{\mathrm{T}}} & \dots & \check{\boldsymbol{\Theta}}^{E^{\mathrm{T}}} & \check{\boldsymbol{\Theta}}^{g1^{\mathrm{T}}} & \check{\boldsymbol{\Theta}}^{g2^{\mathrm{T}}} & \dots & \check{\boldsymbol{\Theta}}^{gE^{\mathrm{T}}} & \check{\boldsymbol{\Theta}}^{g^{\mathrm{T}}} \end{bmatrix}, \end{aligned} \tag{31}$$

and where E is the number of finite element cells and s^e is the e-th element support, i.e.,

$$s^e = \begin{cases} 1 & \text{for } \mathbf{x} \in V^e, \\ 0 & \text{for } \mathbf{x} \notin V^e. \end{cases} \tag{32}$$

The approximation in Eq. (30) is discontinuous across the mesh skeleton. The jump and mean values are approximated in the standard manner

$$[\![\Theta]\!] = [\boldsymbol{\Phi}]\check{\boldsymbol{\Theta}}, \qquad \langle\Theta\rangle = \langle\boldsymbol{\Phi}\rangle\check{\boldsymbol{\Theta}}, \qquad \mathbf{x} \in S_s. \tag{33}$$

In the same way the approximation of the jump and mean values at the distance w from S_s is performed

$$[\![\Theta]\!]_w = [\![\boldsymbol{\Phi}]\!]_w\check{\boldsymbol{\Theta}}, \qquad \langle\Theta\rangle_w = \langle\boldsymbol{\Phi}\rangle_w\check{\boldsymbol{\Theta}}. \tag{34}$$

The kind of approximation presented in this section is flexible and very effective since arbitrary enriching functions can be incorporated into the approximation in the local or global parts of the approximation. In this paper the Galerkin formulation is considered that is why the same approximation as in Eqs. (30) and (33) is applied to the test function v.

In most cases, the local basis functions are polynomials taken from the Taylor expansion. Each polynomial is defined in the e-th cell with the help of local coordinates. In the two-dimensional case the local coordinates (x^e, y^e) are defined in the following way:

$$x^e = \frac{x - x^e_m}{0.5\,h^e_x}, \qquad y^e = \frac{y - y^e_m}{0.5\,h^e_y}. \tag{35}$$

In Eq. (35) the point (x^e_m, y^e_m) is a center of gravity of the e-th element cell and h^e_x, h^e_y are the characteristic lengths of the e-th cell in the x and y directions, respectively. It should be noted that the shape of the triangle and its orientation in respect to x and y axes are arbitrary. It can be noticed that the orientation of local coordinates (x^e, y^e) is the same as global coordinates (x, y). The construction of local coordinates is shown in Fig. 4. The vectors of basis functions of various

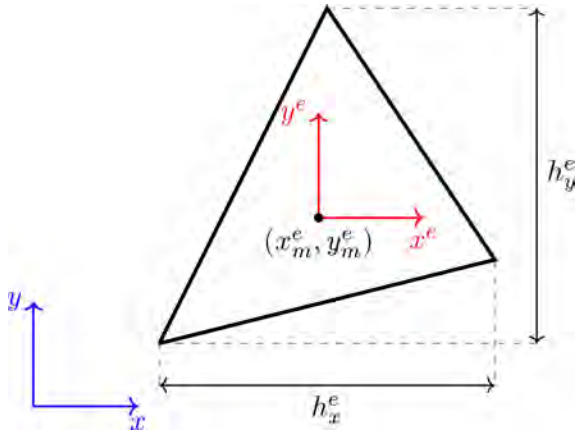

Fig. 4. Construction of local coordinates for the element cell e.

degrees p, used in this paper, are then as follows:

$$\begin{aligned}
&\text{for } p = 1: \quad \mathbf{b}^e = \mathbf{b}^e_1 = \begin{bmatrix} 1 & x^e & y^e \end{bmatrix},\\
&\text{for } p = 2: \quad \mathbf{b}^e = \mathbf{b}^e_2 = \begin{bmatrix} \mathbf{b}^e_1 & x^e y^e & x^{e2} & y^{e2} \end{bmatrix},\\
&\text{for } p = 3: \quad \mathbf{b}^e = \mathbf{b}^e_3 = \begin{bmatrix} \mathbf{b}^e_2 & x^{e3} & x^{e2}y^e & x^e y^{e2} & y^{e3} \end{bmatrix},\\
&\text{for } p = 4: \quad \mathbf{b}^e = \mathbf{b}^e_4 = \begin{bmatrix} \mathbf{b}^e_3 & x^{e4} & x^{e3}y^e & x^{e2}y^{e2} & x^e y^{e3} & y^{e4} \end{bmatrix}.
\end{aligned} \tag{36}$$

In such a way, it is quite easy to define local approximation of arbitrary degree, and the degree may vary among the cells. In the examples presented in this paper the polynomial approximations up to sixth-order (28 basis functions) have been used.

When the approximations from Eqs. (30), (33) and (34) are substituted into the weak form Eq. (24), the linear system of equation is obtained:

$$\mathbf{K}\check{\mathbf{\Theta}} = \mathbf{F}, \tag{37}$$

where

$$\begin{aligned}\mathbf{K} = &\int_V \mathbf{B}^{\mathrm{T}}\mathbf{B}\,\mathrm{d}V + \frac{3}{4}\int_{S_s}\frac{k}{w}[\![\mathbf{\Phi}]\!]^{\mathrm{T}}[\![\mathbf{\Phi}]\!]_w\,\mathrm{d}S - \frac{1}{2}\int_{S_s} k[\![\mathbf{\Phi}]\!]^{\mathrm{T}}\mathbf{n}^{s\mathrm{T}}\langle\mathbf{B}\rangle_w\,\mathrm{d}S \\ &+ 3\int_{S_\Theta}\frac{k}{w}\mathbf{\Phi}^{\mathrm{T}}\mathbf{\Phi}(\mathbf{x}_{2w})\,\mathrm{d}S + 4\int_{S_\Theta} k\,\mathbf{\Phi}^{\mathrm{T}}\mathbf{B}_n(\mathbf{x}_w)\,\mathrm{d}S + \int_{S_\Theta} k\,\mathbf{\Phi}^{\mathrm{T}}\mathbf{B}_n(\mathbf{x}_{2w})\,\mathrm{d}S, \\ \mathbf{F} = &\int_V \mathbf{\Phi}^{\mathrm{T}} r\,\mathrm{d}V - \int_{S_q}\mathbf{\Phi}^{\mathrm{T}}\widehat{h}\,\mathrm{d}S + 3\int_{S_\Theta}\frac{k}{w}\mathbf{\Phi}^{\mathrm{T}}\widehat{\Theta}\,\mathrm{d}S,\end{aligned} \tag{38}$$

where $\mathbf{B} = \nabla\mathbf{\Phi}$ and $\mathbf{B}_n = \nabla_n\mathbf{\Phi}$.

In order to construct the system of equations in Eq. (37) the parameter w has to be evaluated. This value should be small enough so that the FD rules are accurate enough. On the other hand, too small value of w may lead to numerical instabilities. Thus, in the calculations the values of w were set proportional to the characteristic size of finite elements h. In the examples presented in this work this parameter was set $w = h \cdot 10^{-5}$.

5. Examples

In this section, three examples are discussed, which illustrate the approach presented in this paper. In each of the examples the following boundary value problem on a square domain $[-1, 1]\times[-1, 1]$ is considered:

$$\begin{aligned}&-\Delta\Theta = f(x,y),\\ &\Theta = \widehat{\Theta} \quad \text{on} \quad S_\Theta = S,\end{aligned} \tag{39}$$

where the boundary conditions and right-hand side function $f(x,y)$ come from the exact solution $\Theta(x,y)$ that is specific for each of the considered examples. The problem defined in (39) can be seen as a heat flow problem where the thermal conductivity is $k = 1$ and the heat source r is given by the $f(x,y)$ function.

In the first example, the exact solution is a polynomial, the second example deals with an exponential problem and in the third example the trigonometric problem is considered. In the second and third examples, the effects of using non-polynomial local and global basis functions are presented.

In these examples, the error of the approximated solutions is measured. The definition of the error at an arbitrary point in V is defined in the following way:

$$e = \left|\Theta - \overline{\Theta}\right| \qquad \text{in } V, \tag{40}$$

where e is the error of the approximate solution $\overline{\Theta}$, and Θ is the exact solution. In order to measure the global error of the approximate solution the L_2 norm and H_1 semi-norm are used, which are respectively defined as follows

$$\|e\|_{L_2} = \sqrt{\int_V \left(\Theta - \overline{\Theta}\right)^2\,\mathrm{d}V}, \qquad |e|_{H_1} = \sqrt{\int_V \left(\Theta' - \overline{\Theta}'\right)^2\,\mathrm{d}V}. \tag{41}$$

5.1. Polynomial example

In this example the exact solution of the elliptic problem defined in Eq. (39) is given:

$$\Theta(x, y) = x^2 + y^2. \tag{42}$$

In that case the right-hand side function is

$$f(x, y) = -4. \tag{43}$$

At first, the example has been checked whether the DGFD method can reproduce the exact solution for the second-degree local basis functions as well as for the second-degree global functions locally or globally scaled. The exact solution has been obtained in all the approximation configurations. This means that the whole algorithm in the DGFD method is correctly derived and the ideas connected with the approximation method and the FD rules for the compatibility and boundary conditions are correctly applied.

Secondly, the triangular finite elements with first-degree basis functions have been used to show the convergence rate of the DGFD method in the simple example. The results in L_2 norm and H_1 semi-norm are shown in Fig. 5, where *ndof* means number of degrees of freedom and *error* means $\|e\|_{L_2}$ or $|e|_{H_1}$. The convergence rate is typical, which means that in the logarithmic scale the rate is linear in the both error measures.

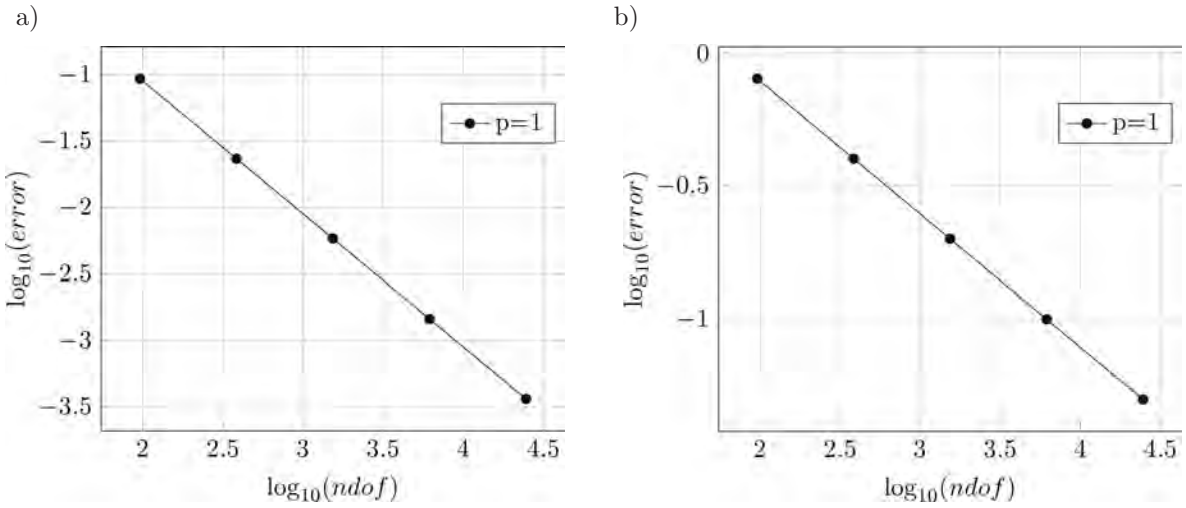

Fig. 5. The convergence of the polynomial example in L_2 norm (a) and H_1 semi-norm (b).

Subsequently, the polynomial example has been solved on the mesh with 128 triangular elements, but using four configurations connected with approximations: firstly all elements have been set as $p = 1$, secondly for the inside elements the order has been set as $p = 2$, thirdly for the inside elements vector $\boldsymbol{\gamma}$ has been set and fourthly for the inside elements vector $\boldsymbol{\beta}$ has been set. Figure 6a shows the approximate solution for the uniform approximation order of $p = 1$. In the next step, the second-order approximation has been applied for the inside cells marked in Fig. 6b. The higher degree approximation for the inside cells has been achieved in three ways: i) by increasing the degrees of local basis function $p = 2$, see Eq. (36), Fig. 6c, ii) by adding the global basis $\boldsymbol{\gamma}$ with the support over those inside cells (Fig. 6b) $\boldsymbol{\gamma} = [x^2 \;\; y^2]$, Fig. 6d and iii) by adding the global basis $\boldsymbol{\beta}$ to the inside cells $\boldsymbol{\beta} = [x^2 \;\; y^2]$, Fig. 6e. The inside elements which have been enriched by higher approximation, Fig. 6b, are chosen to be irregular. This is done intentionally in order to show the flexibility of the proposed approach. We can see in the presented results that in all the cases the final solution is continuous in spite of the fact that the whole approximation is discontinuous on the mesh

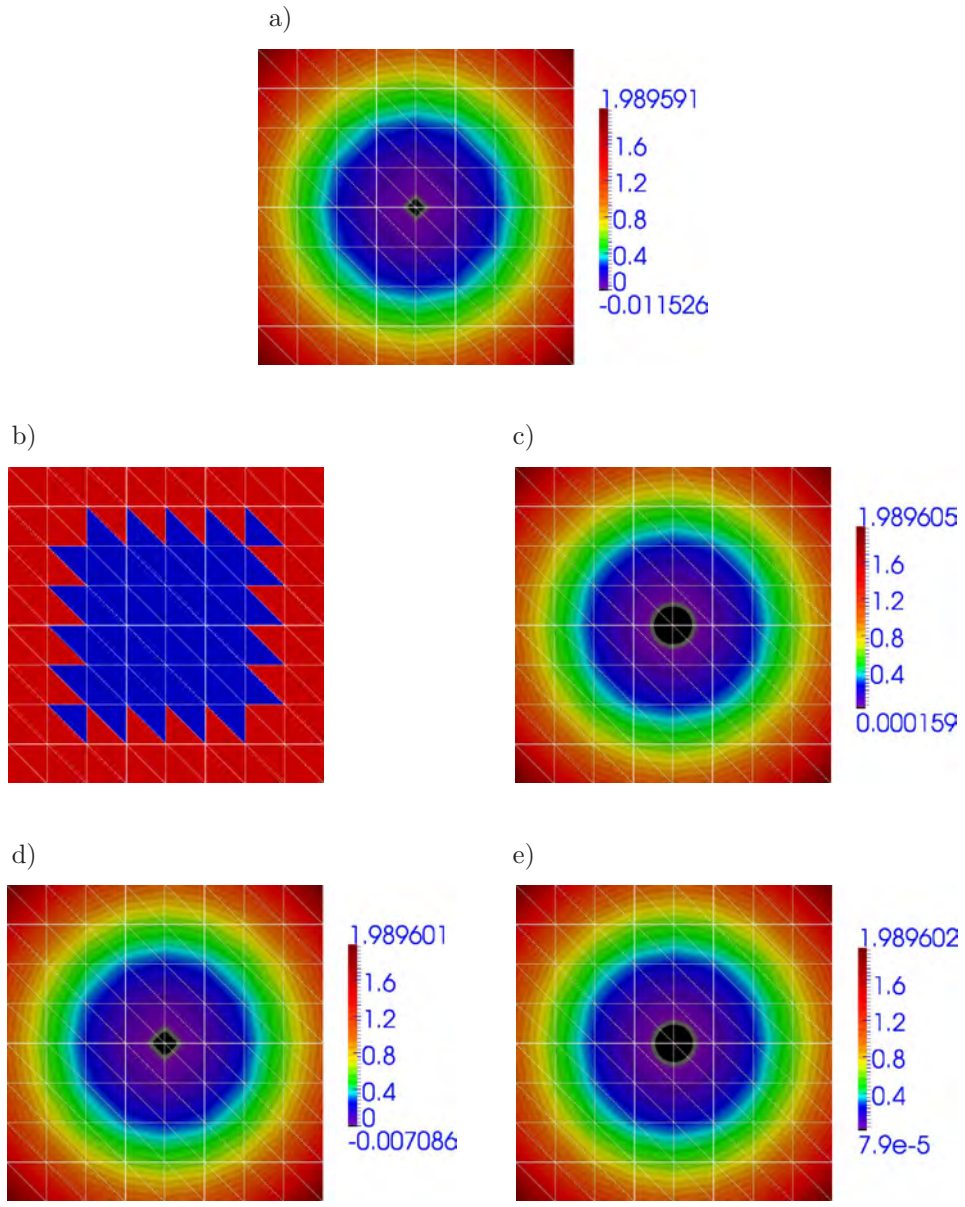

Fig. 6. Approximate solution of polynomial example for the first-order local approximation and enriched inside elements: a) approximate solution with $p = 1$ and 384 $ndof$, b) mesh with marked inside elements where higher order approximation is applied, c) approximate solution where the inside elements have $p = 2$ that gives 534 $ndof$, d) approximate solution where the inside elements have been enriched by $\boldsymbol{\gamma} = [x^2 \;\; y^2]$ that gives 386 $ndof$, e) approximate solution where the inside elements have been enriched by $\boldsymbol{\beta} = [x^2 \;\; y^2]$ that gives 484 $ndof$.

skeleton. Not only the local approximation is discontinuous but also the global approximation causes additional discontinuities. The local-global part of the approximation is discontinuous across the mesh skeleton. Furthermore, the global-global part of the approximation is discontinuous along its support border (in Fig. 6b the border between enriched and regular cells). The presented approach can cope with all those discontinuities and the final results are continuous.

From the results presented in Fig. 6 it is evidently seen that all kinds of approximation proposed in this paper give proper results. However, in this example it can be said that the best results in Figs. 6c, 6d and 6e are obtained when the global-local approximation technique is used, in Fig. 6e the upper and lower values of the approximate solution are the very close to the exact values.

5.2. Exponential example

The exact solution of this example is the following exponential function:

$$\Theta(x,y) = \exp\left(-5(x-y)^2 - 5x^2\right). \tag{44}$$

The function, shown in Fig. 7, has great gradients and that is why it is suitable for numerical tests.

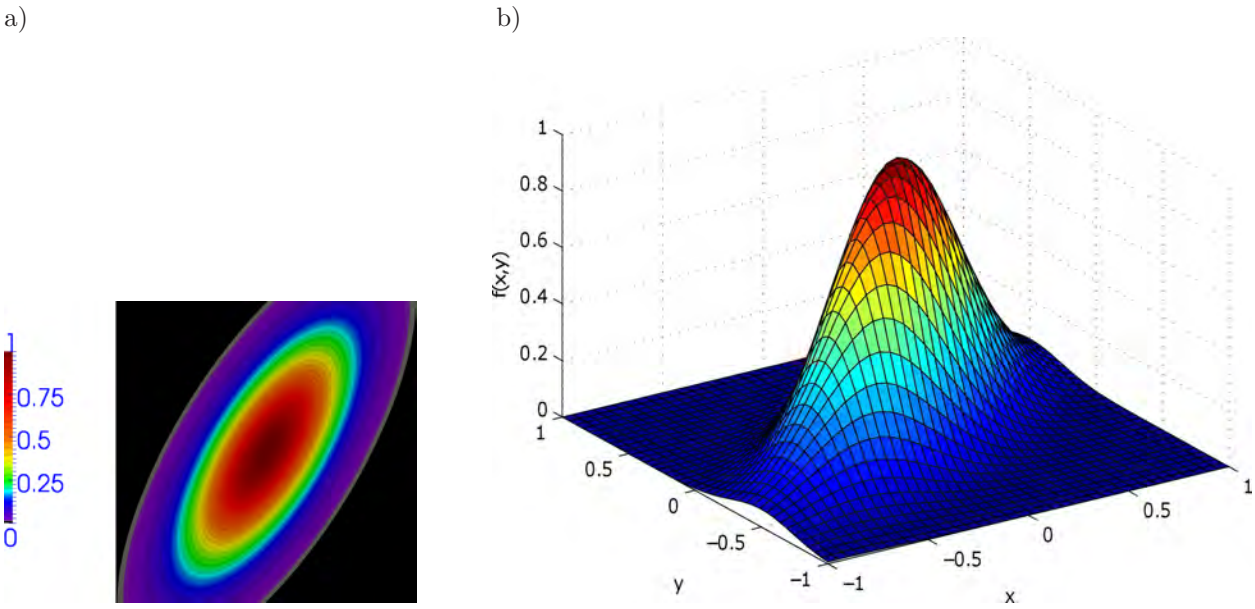

Fig. 7. Exact solution of example no. 2 $\Theta(x,y) = \exp\left(-5(x-y)^2 - 5x^2\right)$.

For the exact solution in Eq. (44) the right-hand side function is as follows:

$$f(x,y) = -\exp\left(-5(x-y)^2 - 5x^2\right)\cdot(20x-10y)^2 + 20\exp\left(-5(x-y)^2 - 5x^2\right) \\ -\exp\left(-5(x-y)^2 - 5x^2\right)\cdot(10x-10y)^2 + 10\exp\left(-5(x-y)^2 - 5x^2\right). \tag{45}$$

The convergence analysis has been performed for the example where only local polynomial approximations are used. Figure 8 shows the convergence of the results obtained by the DGFD

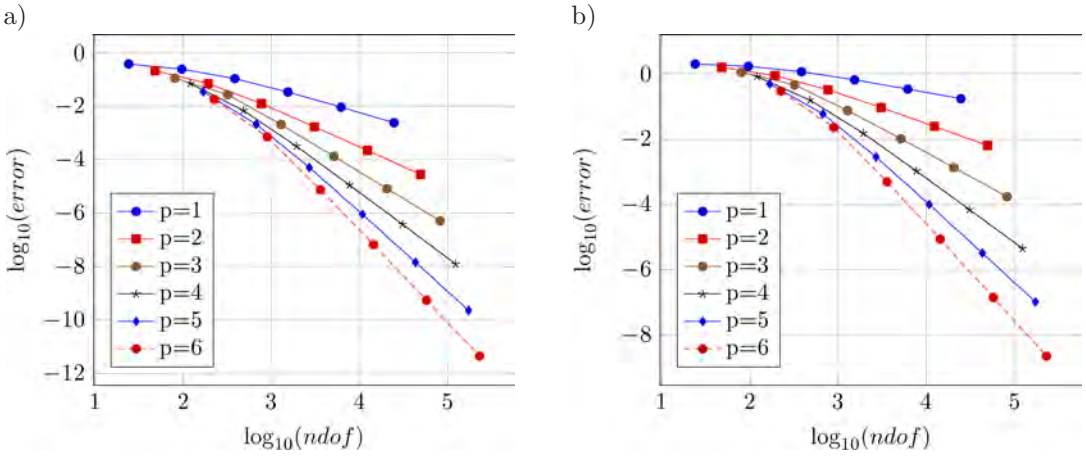

Fig. 8. Convergence analysis of the DGD method in exponential example for various local-local approximation orders. Convergence in L_2 norm (a) and H_1 semi-norm (b).

method for various local-local approximation orders. For comparison, the same convergence analysis has been performed for the SDG method, see Fig. 9. The well-known tendency that for higher degrees approximations higher convergence rates are obtained is observed in the results. This also shows that the DGFD method presented in this paper gives correct results. On the other side, the same rate of convergence is observed for the SDG method, but for higher orders the method stops to converge. In the analyzed problem, the SDG method cannot exceed value 10^{-5} of error in L_2 norm. This shows that the DGFD method is correct and gives more stable results in comparison to the SDG method.

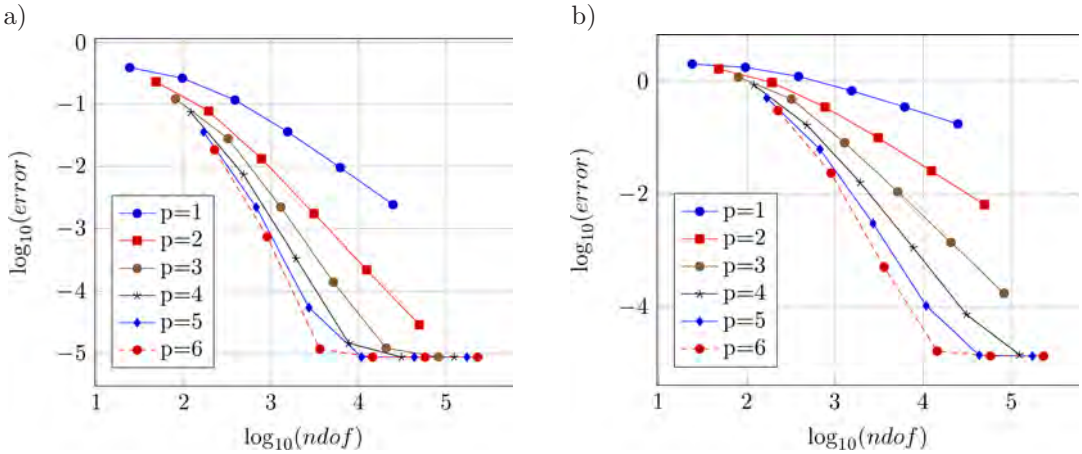

Fig. 9. Convergence analysis of the SDG method in exponential example for various local-local approximation orders. Convergence in L_2 norm (a) and H_1 semi-norm (b).

The exponential example has been solved using standard polynomial local basis function shown in Eq. (36). However, the approach allows one to use other local basis functions. In order to illustrate this property the local exponential functions have been used in the example. In particular, the vector of local basis functions for a triangular cell is in this case as follows:

$$\mathbf{b}^e = \left[\mathbf{b}_2^e \quad \exp(-r_1^2) \quad \exp(-r_2^2) \quad \exp(-r_3^2) \quad \exp(-r_4^2)\right], \tag{46}$$

where $r_i = \sqrt{(x-x_i)^2 + (y-y_i)^2}$ and (x_1, y_1), (x_2, y_2), (x_3, y_3) are the coordinates of the triangle vertices, (x_4, y_4) is the triangle mass centre, and $\mathbf{b}_2^e$ is the vector polynomial basis function taken from Eq. (36). Figure 10a shows the results obtained for the local basis functions from Eq. (46) with 32 finite elements. For comparison, Fig. 10b presents the results for the same mesh but the standard polynomial local basis of $p = 3$ was used, Eq. (36). In both cases, the results are quite satisfactory. This means that in the approach presented in this paper other local basis functions, besides polynomial, can be used. In the next step the convergence analysis has been performed for

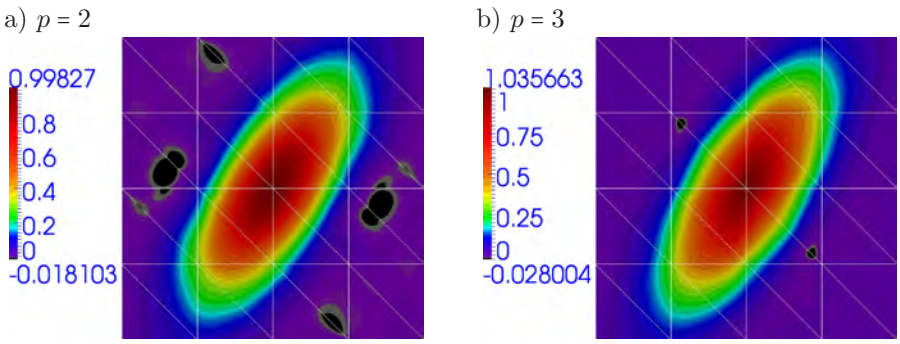

Fig. 10. Solutions of example no. 2 with 32 triangular cells with the polynomial-exponential local basis functions (a) and with standard polynomial local basis (b).

the local basis function from Eq. (46). The results showing the convergence rate for the example, that is, compared with the convergence for the standard polynomial local basis is presented in Fig. 11. In both cases, each cell has the same number of degrees of freedom, namely 10. The results for the mixture polynomial-exponential local basis functions converge in L_2 norm as well as in H_1 semi-norm. However, the rate of convergence is a little bit smaller in comparison to the convergence rate obtained when the standard polynomial basis functions are used. We can conclude here that it is possible, for DGFD, to use non-standard local basis functions and the obtained results are quite correct and still continuous. In general the polynomial basis functions usually give better results in comparison to other basis functions. This comes directly from the Taylor expansion, which says that the polynomial approximation can adjust quite well to arbitrary function.

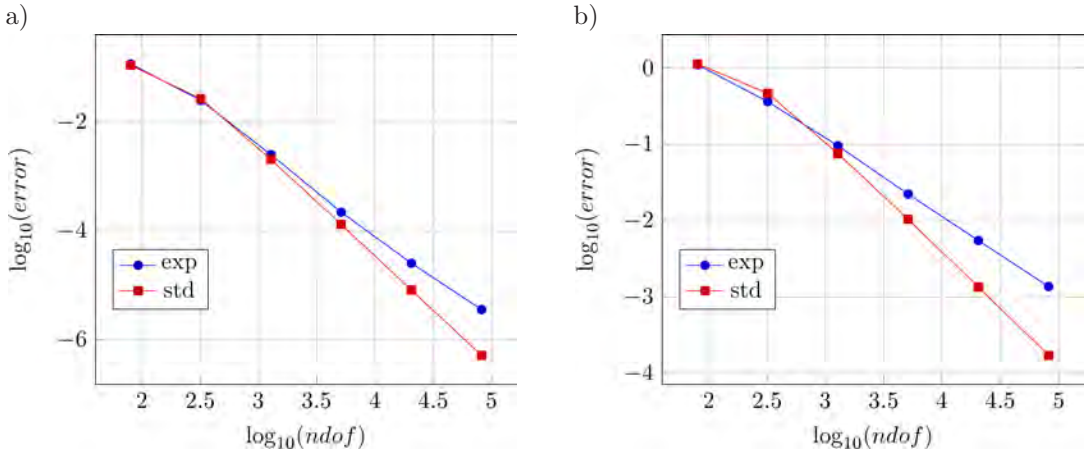

Fig. 11. Convergence in L_2 norm (a) and H_1 semi-norm (b) with polynomial-exponential LB and for comparison with standard LB of order $p = 3$.

5.3. Trigonometric example

In the third example, we consider the trigonometric problem for which the exact solution is

$$\Theta(x, y) = x^2\, y + \sin(2\,\pi\, x)\, \sin(2\,\pi\, y), \tag{47}$$

and the right-hand side function is

$$f(x, y) = -2y + 8\,\pi^2\, \sin(2\,\pi\, x)\, \sin(2\,\pi\, y). \tag{48}$$

The exact solution from Eq. (47) is depicted in Fig. 12. We can see that the exact solution fluctuates and has many peaks in the considered domain. In this example, the combination of

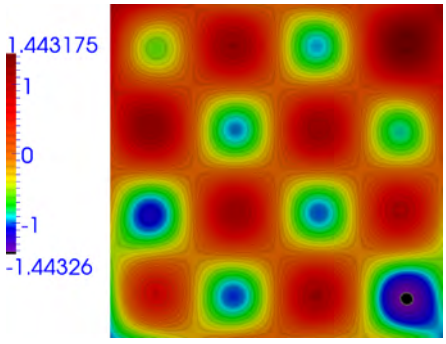

Fig. 12. Exact solution for example no. 3.

local-local, global-local and global-global approximations has been used with the following basis functions

$$\begin{aligned}
\mathbf{b}^e &= \begin{bmatrix} 1 & x^e & y^3 & x^e y^e & x^{e2} & y^{e2} \end{bmatrix}, \\
\boldsymbol{\beta} &= \begin{bmatrix} \sin(2\pi x) & \sin(2\pi y) & \cos(2\pi x) & \cos(2\pi y) \end{bmatrix}, \\
\boldsymbol{\gamma} &= \begin{bmatrix} x^3 & x^2 y & x y^2 & y^3 \end{bmatrix}.
\end{aligned} \tag{49}$$

All the global functions in $\boldsymbol{\beta}$ and $\boldsymbol{\gamma}$ are spanned over all elements in the domain.

The calculations have been performed for meshes with 32, 128 and 512 triangular cells. In this example, the DGFD method has been used in the version presented in Sec. 4 where the fourth-degree FD relations on the skeleton and outer boundary are used (case 1). For comparison, the example has been solved by another version of the DGFD method where on the skeleton the second-degree and on the outer boundary the first-degree finite difference relations are used (case 2). In order to see the difference between the approach presented in this paper and the SDG method, the same example has been calculated by the standard approach (case 3).

The results are presented in the form of maps of the obtained approximate solution and maps of the solution error. Figures 13–15 show the results for the 32-element mesh. For the 128-element mesh the results are presented in Figs. 16–18. Finally, the results for the mesh with 512 elements are shown in Figs. 19–21.

The results show that case 1 has given the best solution for each of the meshes. On the other hand, the SDG method has given the worst results. This means that the DGFD method generally gives better results than the SDG method even if a low degree FD compatibility and boundary conditions are used. For the coarse mesh, the DGFD method gives discontinuous solution, Figs. 13 and 14, but on the other hand the obtained result is closer to the exact solution in comparison to

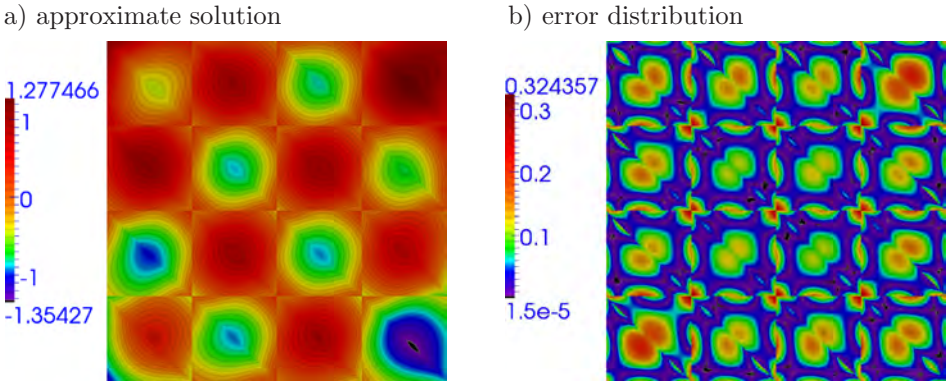

Fig. 13. Solution and error for example no. 3 with high degree FD (case 1) on 32 triangular cell mesh.

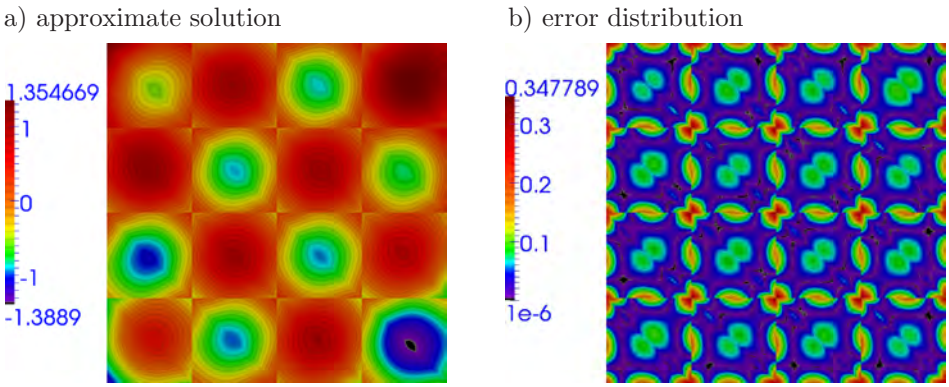

Fig. 14. Solution and error for example no. 3 with low degree FD (case 2) on 32 triangular cell mesh.

a) approximate solution b) error distribution

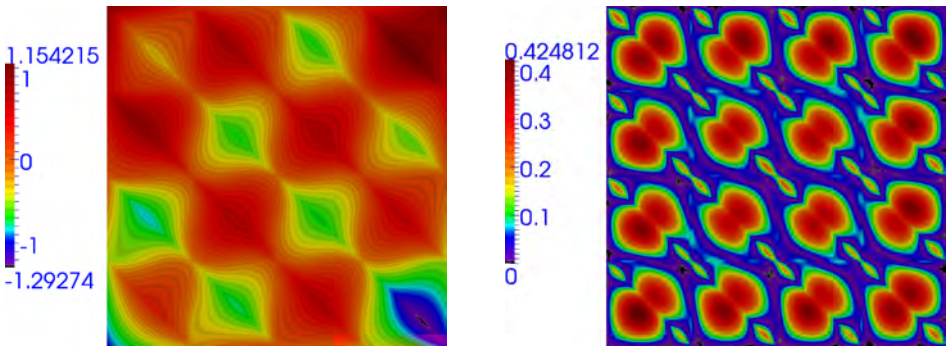

Fig. 15. Solution and error for example no. 3 by SDG (case 3) on 32 triangular cell mesh.

a) approximate solution b) error distribution

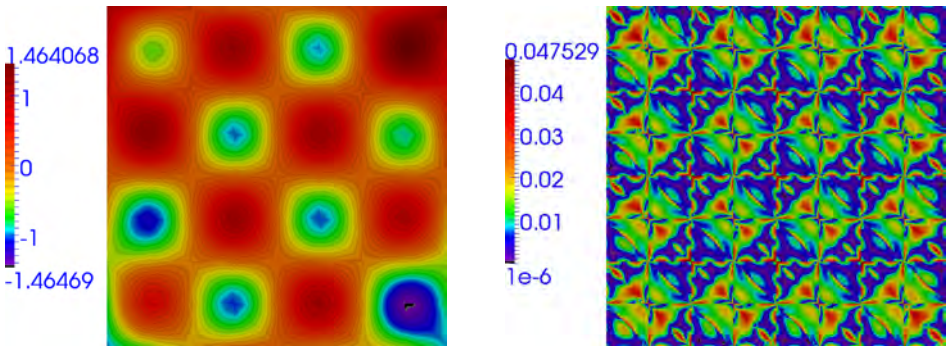

Fig. 16. Solution and error for example no. 3 with high degree FD (case 1) on 128 triangular cell mesh.

a) approximate solution b) error distribution

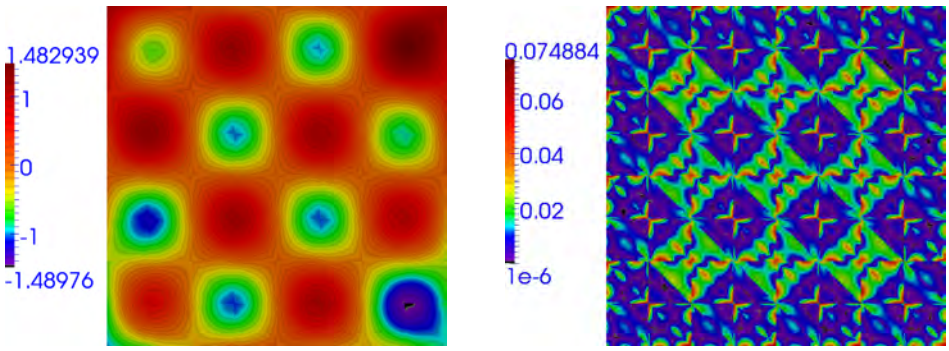

Fig. 17. Solution and error for example no. 3 with low degree FD (case 2) on 128 triangular cell mesh.

a) approximate solution b) error distribution

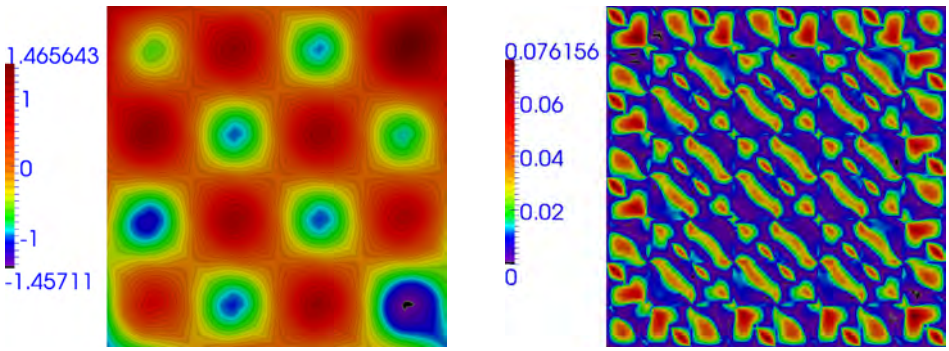

Fig. 18. Solution and error for example no. 3 by SDG (case 3) on 128 triangular cell mesh.

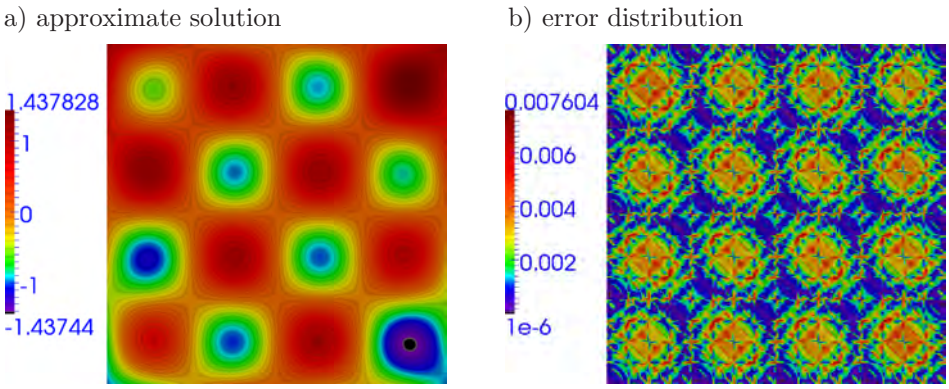

Fig. 19. Solution and error for example no. 3 with high degree FD (case 1) on 512 triangular cell mesh.

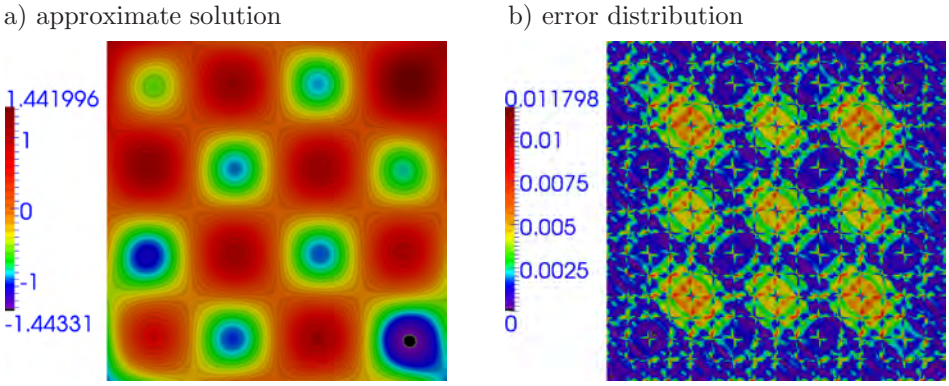

Fig. 20. Solution and error for example no. 3 with low degree FD (case 2) on 512 triangular cell mesh.

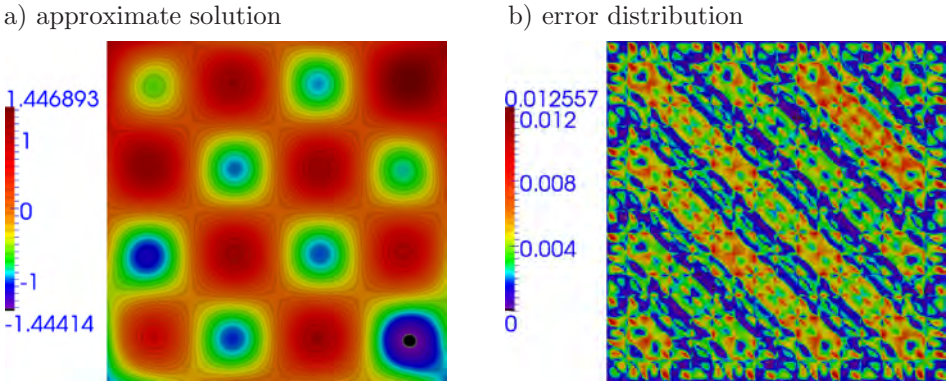

Fig. 21. Solution and error for example no. 3 by SDG (case 3) on 512 triangular cell mesh.

the standard approach, Fig. 15. For dense meshes in each of cases the results have been continuous but still the DGFD method has given smaller errors in comparison to the SDG method.

6. Conclusions

The DGFD method has been presented in this paper. The approximation field in this method is discontinuous and the compatibility condition that stitches together the approximations, is based on the FD relations. Although the FD relations can generally be of arbitrary degree, in this paper the second and fourth-degree has been used. Quite similar approach is used to enforce Dirichlet boundary conditions and in this case the first, second or fourth degree FD relations have been applied.

In the DGFD method there are no shape functions, instead arbitrary basis functions can be used. The basis functions are usually polynomials which are defined in the local coordinates associated with each finite element. In this paper, the exponential basis functions are also used. The basis functions associated with the cells are called local basis functions. Next to the local basis functions also the global functions can be used in the presented approach. The global basis functions can be locally scaled (i.e., in each cells additional degrees of freedom are associated with those functions) or globally scaled (i.e., the degrees of freedom are associated with the whole mesh). In consequence, three types of approximations can be combined: local-local, global-local and global-global.

The main advantage of the DGFD method is the fact that this method is stable even for high-order finite elements and gives better results in comparison to the standard DG method. Due to the fact that the mixed approximation techniques can be applied with quite arbitrary basis functions the DGFD method can be easily enriched with some special functions, i.e., sinusoidal basis functions in places where solution has trigonometrical character, etc. Two elements of different orders can be set side by side. This does not need the hierarchical shape functions, as used in the FEM [14, 53, 54] [A, B, C] and other DG approaches [27, 28, 40]. Instead the mesh skeleton has to be included in the method formulation. As a disadvantage of the DGFD method the fact that due to compatibility conditions the main matrix in this method is not symmetric can be pointed out. The computational costs of the DGFD method are of the same level as in the standard DG method.

The presented approach is illustrated with a couple of two-dimensional examples where the correctness, effectiveness and flexibility of the DGFD method have been shown. Although the presented examples are two-dimensional, the approach can be directly applied to full three-dimensional problems. In this paper, the scalar elliptical problem is studied. However, the approach is also suitable for other kinds of problems.

Appendix A

In this paper, the FD relations differ from the standard approach. Appendix A presents the detailed derivation of the FD relations applied in this paper. In general, the FD equations show how to calculate approximately the derivatives of a certain function with the help of discrete values of the function. In the approach applied in this paper not only discrete values of the function but also its discrete derivatives are used to derive the FD equations. In Appendix the appropriate relations are firstly derived for the mid-point, i.e., we calculate the derivatives at the point in the middle of the regarded domain. Secondly, for the point located on the right side of the domain, what is connected with the fact that the normal to outer boundary goes out of the domain.

A.1. Finite difference rules to calculate derivatives at the middle node

There is a function g and the values of the function are known at all nodes presented in Fig. A1: $g(-h)$, $g(0)$ and $g(h)$. Additionally the first derivatives of the function are known at the nodes except the node at the origin: $g'(-h)$ and $g'(h)$. The task is to calculate the first derivative of the function at the origin: $g'(0) = ?$. However, in the presented approach other derivatives are also calculated at the origin. This is done using the Taylor expansion up to the second or fourth degree.

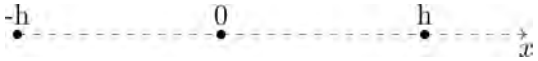

Fig. A1. Nodes to calculate derivatives at the middle point using second-order or fourth-order FD rule.

To obtain the second-order approximation, the Taylor expansion for $g(h)$ and $g(-h)$ truncated after the second-order term is written as

$$g(h) = g(0) + g'(0)\,h + \frac{1}{2}g''(0)\,h^2, \qquad g(-h) = g(0) - g'(0)\,h + \frac{1}{2}g''(0)\,h^2. \tag{A1}$$

Equations (A1) are rearranged so that the following system of equations is constructed:

$$\begin{bmatrix} 1 & \frac{1}{2}h \\ -1 & \frac{1}{2}h \end{bmatrix} \begin{bmatrix} g'(0) \\ g''(0) \end{bmatrix} = \begin{bmatrix} \frac{g(h)-g(0)}{h} \\ \frac{g(-h)-g(0)}{h} \end{bmatrix}. \tag{A2}$$

The solution of Eq. (A2) gives the FD rules for the first and second derivatives at the origin

$$\begin{aligned} g'(0) &= \frac{1}{2h}\left(g(h)-g(-h)\right), \\ g''(0) &= \frac{1}{h^2}\left(g(h)-2g(0)+g(-h)\right). \end{aligned} \tag{A3}$$

In the fourth-degree approximation, the Taylor expansion at points h and $-h$ is performed for the function and its first derivative, which are truncated after fourth or third order, respectively. This gives the following approximations:

$$\begin{aligned} g(h) &= g(0) + g'(0)\,h + \frac{1}{2}g''(0)\,h^2 + \frac{1}{6}g'''(0)\,h^3 + \frac{1}{24}g^{IV}(0)\,h^4, \\ g'(h) &= g'(0) + g''(0)\,h + \frac{1}{2}g'''(0)\,h^2 + \frac{1}{6}g^{IV}h^3, \\ g(-h) &= g(0) - g'(0)\,h + \frac{1}{2}g''(0)\,h^2 - \frac{1}{6}g'''(0)\,h^3 + \frac{1}{24}g^{IV}(0)\,h^4, \\ g'(-h) &= g'(0) - g''(0)\,h + \frac{1}{2}g'''(0)\,h^2 - \frac{1}{6}g^{IV}h^3. \end{aligned} \tag{A4}$$

After rearrangement of Eqs. (A4) the system of equations is obtained:

$$\begin{bmatrix} 1 & \frac{1}{2}h & \frac{1}{6}h^2 & \frac{1}{24}h^3 \\ 1 & h & \frac{1}{2}h^2 & \frac{1}{6}h^3 \\ -1 & \frac{1}{2}h & -\frac{1}{6}h^2 & \frac{1}{24}h^3 \\ 1 & -h & \frac{1}{2}h^2 & -\frac{1}{6}h^3 \end{bmatrix} \begin{bmatrix} g'(0) \\ g''(0) \\ g'''(0) \\ g^{IV}(0) \end{bmatrix} = \begin{bmatrix} \frac{g(h)-g(0)}{h} \\ g'(h) \\ \frac{g(-h)-g(0)}{h} \\ g'(-h) \end{bmatrix}. \tag{A5}$$

After solving Eq. (A5) we obtain the derivatives of function g at the origin:

$$\begin{aligned} g'(0) &= \frac{3}{4h}\left(g(h)-g(-h)\right) - \frac{1}{4}\left(g'(h)+g'(-h)\right), \\ g''(0) &= \frac{2}{h^2}\left(g(-h)-2g(0)+g(h)\right) - \frac{1}{2h}\left(g'(h)-g'(-h)\right), \\ g'''(0) &= \frac{3}{2h^3}\left(g(-h)-g(h)\right) + \frac{1}{2h^2}\left(g'(h)+g'(-h)\right), \\ g^{IV}(0) &= \frac{12}{h^4}\left(-g(-h)+2g(0)-g(h)\right) + \frac{6}{h^3}\left(g'(h)-g'(-h)\right). \end{aligned} \tag{A6}$$

A.2. Finite difference rules to calculate derivatives at right node

The derivatives of the function g at the origin have to be evaluated, but now the three nodes are located as shown in Fig. A2. It is assumed that the values of the considered functions are known at those nodes, i.e. $g(-2h)$, $g(-h)$, $g(0)$. Additionally, the first derivatives at the first two nodes are known, i.e., $g'(-2h)$, $g'(-h)$.

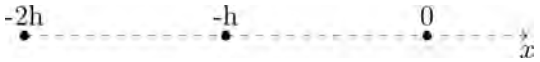

Fig. A2. Nodes to calculate derivatives at end-point using first-order, second-order or fourth-order FD rule.

The derivatives at the origin are evaluated using the Taylor expansion of first, second or fourth order. In the simplest, first-degree case the Taylor expansion at point $-h$ is performed:

$$g(-h) = g(0) - g'(0)\,h. \tag{A7}$$

This directly gives the first-degree FD scheme:

$$g'(0) = \frac{1}{h}\left(g(0) - g(-h)\right). \tag{A8}$$

In order to obtain the second-degree evaluation the following Taylor expansions are used:

$$\begin{aligned} g(-h) &= g(0) - g'(0)\,h + \frac{1}{2}g''(0)\,h^2, \\ g'(-h) &= g'(0) - g''(0)\,h. \end{aligned} \tag{A9}$$

Equations (A9) are rewritten to get the system of equations in matrix notation:

$$\begin{bmatrix} 1 & -\frac{1}{2}h \\ 1 & -h \end{bmatrix} \begin{bmatrix} g'(0) \\ g''(0) \end{bmatrix} = \begin{bmatrix} \dfrac{g(0) - g(-h)}{h} \\ g'(-h) \end{bmatrix}. \tag{A10}$$

Solution of Eq. (A10) gives the FD relations for the first and second derivatives at the origin:

$$\begin{aligned} g'(0) &= \frac{2}{h}\left(g(0) - g(-h)\right) - g'(-h), \\ g''(0) &= \frac{2}{h^2}\left(g(0) - g(-h)\right) - \frac{2}{h}g'(-h). \end{aligned} \tag{A11}$$

Consequently, in order to find the derivatives at the origin on the basis of the fourth-degree approximation the following Taylor expansions are used:

$$\begin{aligned} g(-h) &= g(0) - g'(0)\,h + \frac{1}{2}g''(0)\,h^2 - \frac{1}{6}g'''(0)\,h^3 + \frac{1}{24}g^{IV}(0)\,h^4, \\ g'(-h) &= g'(0) - g''(0)\,h + \frac{1}{2}g'''(0)\,h^2 - \frac{1}{6}g^{IV}(0)\,h^3, \\ g(-2h) &= g(0) - g'(0)\,(2h) + \frac{1}{2}g''(0)\,(2h)^2 - \frac{1}{6}g'''(0)\,(2h)^3 - + \frac{1}{24}g^{IV}(0)\,(2h)^4, \\ g'(-2h) &= g'(0) - g''(0)\,(2h) + \frac{1}{2}g'''(0)\,(2h)^2 - \frac{1}{6}g^{IV}(0)\,(2h)^3. \end{aligned} \tag{A12}$$

The reformatted Eqs. (A12) in matrix notation read a

$$\begin{bmatrix} 1 & -\frac{1}{2}h & \frac{1}{6}h^2 & -\frac{1}{24}h^3 \\ 1 & -h & \frac{1}{2}h^2 & -\frac{1}{6}h^3 \\ 1 & -\frac{1}{2}(2h) & \frac{1}{6}(2h)^2 & -\frac{1}{24}(2h)^3 \\ 1 & -2h & \frac{1}{2}(2h)^2 & -\frac{1}{6}(2h)^3 \end{bmatrix} \begin{bmatrix} g'(0) \\ g''(0) \\ g'''(0) \\ g^{IV}(0) \end{bmatrix} = \begin{bmatrix} \frac{g(0)-g(-h)}{h} \\ g'(-h) \\ \frac{g(0)-g(-2h)}{2h} \\ g'(-2h) \end{bmatrix}. \tag{A13}$$

Solution of Eq. (A13) gives the fourth-degree FD rules for the derivatives at the origin

$$\begin{aligned} g'(0) &= \frac{3}{h}\left(g(0)-g(-2h)\right) - 4\,g'(-h) - g'(2h), \\ g''(0) &= \frac{1}{2h^2}\left(-29\,g(-2h) + 16\,g(-h) + 13\,g(0)\right) - \frac{1}{h}\left(16\,g'(-h) + 5\,g'(-2h)\right), \\ g'''(0) &= \frac{3}{h^3}\left(-11\,g(-2\,h) + 8\,g(-h) + 3\,g(0)\right) - \frac{3}{h^2}\left(4\,g'(-2h) + 10\,g(-h)\right), \\ g^{IV}(0) &= \frac{6}{h^4}\left(-5\,g(-2\,h) + 4\,g(-h) + g(0)\right) - \frac{12}{h^3}\left(g'(-2h) + 2\,g(-h)\right). \end{aligned} \tag{A14}$$

Acknowledgement

This research has been supported by the project "Cracow University of Technology development program – the top quality teaching for the prospective Polish engineers: University of the 21st century", number POKL.04.01.01-00-029/10-00. The project has been co-financed by the European Union within the confines of the European Social Fund, and realized under the auspices of the Polish Ministry of Science and Higher Education.

References

[1] D.N. Arnold. An interior penalty finite element method with discontinuous elements. *SIAM J. Numer. Anal.*, **19**(4): 175–186, 1982.

[2] D.N. Arnold, F. Brezzi, B. Cockburn, L.D. Marini. Unified analysis of discontinuous Galerkin methods for elliptic problems. *SIAM J. Numer. Anal.*, **39**(5): 1749–1779, May 2001.

[3] I. Babuška, J.M. Melenk. The partition of unity method. *International Journal for Numerical Methods in Engineering*, **40**(4): 727–758, 1997.

[4] G. Billet, J. Ryan. A Runge-Kutta discontinuous Galerkin approach to solve reactive flows: The hyperbolic operator. *Journal of Computational Physics*, **230**(4): 1064–1083, 2011.

[5] S. Brogniez, C. Farhat, E. Hachem. A high-order discontinuous Galerkin method with Lagrange multipliers for advection-diffusion problems. *Computer Methods in Applied Mechanics and Engineering*, **264**: 49–66, 2013.

[6] T. Bui-Thanh, O. Ghattas. Analysis of an *hp*-nonconforming discontinuous Galerkin spectral element method for wave propagation. *SIAM Journal on Numerical Analysis*, **50**(3): 1801–1826, 2012.

[7] N.K. Burgess, D.J. Mavriplis. *hp*-adaptive discontinuous Galerkin solver for the Navier-Stokes equations. *American Institute of Aeronautics and Astronautics*, **50**(12): 2682–2692, 2012.

[8] Y. Chen, J. Huang, Y. Huang, Y. Xu. On the local discontinuous Galerkin method for linear elasticity. *Mathematical Problems in Engineering*, p. 20, 2010.

[9] B. Cockburn, S. Hou, C-W. Shu. The Runge-Kutta local projection discontinuous Galerkin finite element method for conservation laws. IV: The multidimensional case. *Mathematics of Computation*, **54**: 545–581, 1990.

[10] B. Cockburn, S. Lin, C-W. Shu. TVB Runge-Kutta local projection discontinuous Galerkin finite element method for conservation laws. III: One-dimensional systems. *Journal of Computational Physics*, **84**(1): 90–113, 1989.

[11] B. Cockburn, C-W. Shu. TVB Runge-Kutta local projection discontinuous Galerkin finite element method for conservation laws. II. General framework. *Mathematics of Computation*, **52**(186): 411–435, 1989.

[12] B. Cockburn, C-W. Shu. The local discontinuous Galerkin method for time-dependent convection-diffusion systems. *SIAM Journal on Numerical Analysis*, **35**(6): 2440–2463, 1998.

[13] C. Dawson, Sh. Sun, M.F. Wheeler. Compatible algorithms for coupled flow and transport. *Computer Methods in Applied Mechanics and Engineering*, **193**(23–26): 2565–2580, 2004.

[14] L. Demkowicz. *Computing with hp-ADAPTIVE FINITE ELEMENTS: Volume 1 One and Two Dimensional Elliptic and Maxwell Problems*. Chapman & Hall/CRC Applied Mathematics & Nonlinear Science. CRC Press, 2006.

[15] P.N. Dorival, B.P.S. Persival. Generalized finite element method in linear and nonlinear structural dynamic analyses. *Engineering Computations*, **33**(3): 806–830, 2016.

[16] M. Elliotis, G. Georgiou, Ch. Xenophontos. Solving Laplacian problems with boundary singularities: a comparison of a singular function boundary integral method with the p/hp version of the finite element method. *Applied Mathematics and Computation*, **169**(1): 485–499, 2005.

[17] G. Engel, K. Garikipati, T.J.R. Hughes, M.G. Larson, L. Mazzei, R.L. Taylor. Continuous/discontinuous finite element approximations of fourth-order elliptic problems in structural and continuum mechanics with applications to thin beams and plates, and strain gradient elasticity. *Computer Methods in Applied Mechanics and Engineering*, **191**(34): 3669–3750, 2002.

[18] Y. Epshteyn, B. Rivire. Analysis of discontinuous Galerkin methods for incompressible two-phase flow. *Journal of Computational and Applied Mathematics*, **225**(2): 487–509, 2009.

[19] Ch. Farhat, I. Harari, U. Hetmaniuk. A discontinuous Galerkin method with Lagrange multipliers for the solution of Helmholtz problems in the mid-frequency regime. *Computer Methods in Applied Mechanics and Engineering*, **192**(11–12): 1389–1419, 2003.

[20] D. Fournier, R. Herbin, R. Tellier. Discontinuous Galerkin discretization and *hp*-refinement for the resolution of the neutron transport equation. *SIAM Journal on Scientific Computing*, **35**(2): A936–A956, 2013.

[21] E. Georgoulis, E. Hall, P. Houston. Discontinuous Galerkin methods for advection-diffusion-reaction problems on anisotropically refined meshes. *SIAM Journal on Scientific Computing*, **30**(1): 246–271, 2008.

[22] C. Gürkan, E. Sala-Lardies, M. Kronbichler, S. Fernández-Méndez. *eXtended Hybridizable Discontinuous Galerkin (X-HDG) for Void and Bimaterial Problems*, pp. 103–122. Springer International Publishing, Cham, 2016.

[23] P. Hansbo, M.G. Larson. Discontinuous Galerkin methods for incompressible and nearly incompressible elasticity by Nitsche's method. *Computer Methods in Applied Mechanics and Engineering*, **191**(17–18): 1895–1908, 2002.

[24] J. Jaśkowiec. The *hp* nonconforming mesh refinement based on Zienkiewicz-Zhu error estimation in discontinuous Galerkin finite element method. *Computer Assisted Methods in Engineering and Science*, **23**(1): 43–67, 2016.

[25] J. Jaśkowiec, F.P. van der Meer. A consistent iterative scheme for 2D and 3D cohesive crack analysis in XFEM. *Computers & Structures*, **136**: 98–107, 2014.

[26] L. Ji, Y. Xu. Optimal error estimates of the local discontinuous Galerkin method for surface diffusion of graphs on cartesian meshes. *J. Sci. Comput.*, **51**(1): 1–27, April 2012.

[27] H. Kaneko, K.S. Bey, G.J.W. Hou. A discontinuous Galerkin method for parabolic problems with modified *hp*-finite element approximation technique. *Applied Mathematics and Computation*, **182**(2): 1405–1417, 2006.

[28] H. Kaneko, K.S. Bey, Y. Lenbury, P. Toghaw. Numerical experiments using hierarchical finite element method for nonlinear heat conduction in plates. *Applied Mathematics and Computation*, **201**(1–2): 414–430, 2008.

[29] M-Y. Kim. A discontinuous Galerkin method with Lagrange multiplier for hyperbolic conservation laws with boundary conditions. *Computers & Mathematics with Applications*, **70**(4): 488–506, 2015.

[30] F. Kummer. Extended discontinuous Galerkin methods for two-phase flows: the spatial discretization. *International Journal for Numerical Methods in Engineering*, **109**(2): 259–289, 2017.

[31] D. Kuzmin. A vertex-based hierarchical slope limiter for p-adaptive discontinuous Galerkin methods. *Journal of Computational and Applied Mathematics*, **233**(12): 3077–3085, 2010.

[32] H. Luo, J.D. Baum, R. Löhner. A discontinuous Galerkin method based on a Taylor basis for the compressible flows on arbitrary grids. *Journal of Computational Physics*, **227**(20): 8875–8893, 2008.

[33] H. Luo, L. Luo, R. Nourgaliev, V.A. Mousseau, N. Dinh. A reconstructed discontinuous Galerkin method for the compressible Navier-Stokes equations on arbitrary grids. *Journal of Computational Physics*, **229**(19): 6961–6978, 2010.

[34] J.M. Melenk, I. Babuška. The partition of unity finite element method: Basic theory and applications. *Computer Methods in Applied Mechanics and Engineering*, **139**(1–4): 289–314, 1996.

[35] N. Moës, T. Belytschko. Extended finite element method for cohesive crack growth. *Engineering Fracture Mechanics*, **69**(7): 813–833, 2002.

[36] N.C. Nguyen, J. Peraire, B. Cockburn. *Hybridizable Discontinuous Galerkin Methods*, pp. 63–84. Springer Berlin Heidelberg, Berlin, Heidelberg, 2011.

[37] J. Nitsche. Über ein Variationsprinzip zur Lösung von Dirichlet-Problemen bei Verwendung von Teilräumen, die keinen Randbedingungen unterworfen sind. *Abhandlungen aus dem Mathematischen Seminar der Universität Hamburg*, **36**(1): 9–15, 1971.
[38] D.A. Di Pietro, S. Nicaise. A locking-free discontinuous Galerkin method for linear elasticity in locally nearly incompressible heterogeneous media. *Applied Numerical Mathematics*, **63**: 105–116, 2013.
[39] W.H. Reed, T.R. Hill. *Triangular Mesh Methods for the Neutron Transport Equation*. Los Alamos Scientific Laboratory Report LA-UR-73-479, 1973.
[40] B. Riviére. *Discontinuous Galerkin Methods for Solving Elliptic and Parabolic Equations: Theory and Implementation*. Frontiers in Applied Mathematics. Society for Industrial and Applied Mathematics, 2008.
[41] B. Riviére, M.F. Wheeler, K. Banaś. Part II. Discontinuous Galerkin method applied to a single phase flow in porous media. *Computational Geosciences*, **4**(4): 337–349, 2000.
[42] B. Riviére, M. Wheeler, V. Girault. A priori error estimates for finite element methods based on discontinuous approximation spaces for elliptic problems. *SIAM Journal on Numerical Analysis*, **39**(3): 902–931, 2001.
[43] Y. Shen, A. Lew. Stability and convergence proofs for a discontinuous-Galerkin-based extended finite element method for fracture mechanics. *Computer Methods in Applied Mechanics and Engineering*, **199**(37–40): 2360–2382, 2010.
[44] Y. Shen, A.J. Lew. A locking-free and optimally convergent discontinuous-Galerkin-based extended finite element method for cracked nearly incompressible solids. *Computer Methods in Applied Mechanics and Engineering*, **273**: 119–142, 2014.
[45] F. Stan. Discontinuous Galerkin method for interface crack propagation. *International Journal of Material Forming*, **1**(1): 1127–1130, 2008.
[46] T. Strouboulis, I. Babuška, K. Copps. The design and analysis of the generalized finite element method. *Computer Methods in Applied Mechanics and Engineering*, **181**(1–3): 43–69, 2000.
[47] T. Strouboulis, K. Copps, I. Babuška. The generalized finite element method. *Computer Methods in Applied Mechanics and Engineering*, **190**(32–33): 4081–4193, 2001.
[48] I. Toulopoulos. An interior penalty discontinuous Galerkin finite element method for quasilinear parabolic problems. *Finite Elements in Analysis and Design*, **95**: 42–50, 2015.
[49] F. Vilar, P-H. Maire, R. Abgrall. A discontinuous Galerkin discretization for solving the two-dimensional gas dynamics equations written under total Lagrangian formulation on general unstructured grids. *Journal of Computational Physics*, **276**: 188–234, 2014.
[50] M. Wheeler. An elliptic collocation-finite element method with interior penalties. *SIAM Journal on Numerical Analysis*, **15**(1): 152–161, 1978.
[51] Y. Xia, H. Luo, M. Frisbey, R. Nourgaliev. A set of parallel, implicit methods for a reconstructed discontinuous Galerkin method for compressible flows on 3D hybrid grids. *Computers & Fluids*, **98**: 134–151, 2014.
[52] L. Yuan, C-W. Shu. Discontinuous Galerkin method based on non-polynomial approximation spaces. *Journal of Computational Physics*, **218**(1): 295–323, 2006.
[53] G. Zboiński, L. Demkowicz. *Application of the 3D hpq Adaptive Finite Element for Plate and Shell Analysis*. Technical Report TICAM Report 94-13, Texas Institute for Computational and Applied Mathematics. The University of Texas at Austin, Austin (Texas), 1994.
[54] G. Zboinski. Adaptive *hpq* finite element methods for the analysis of 3D-based models of complex structures. Part 1. Hierarchical modeling and approximations. *Computer Methods in Applied Mechanics and Engineering*, **199**(45–48): 2913–2940, 2010.
[55] Q. Zhang, C-W. Shu. Stability analysis and a priori error estimates of the third order explicit Runge-Kutta discontinuous Galerkin method for scalar conservation laws. *SIAM J. Numer. Anal.*, **48**(3): 1038–1063, July 2010.
[56] T. Zhang, Sh. Yu. The derivative patch interpolation recovery technique and superconvergence for the discontinuous Galerkin method. *Applied Numerical Mathematics*, **85**: 128–141, 2014.